

# Structural Features Involved in the Formation of a Complex between the Monomeric or the Dimeric Form of the Rev-erb $\beta$ DNA-Binding Domain and Its DNA Reactive Sites<sup>†,‡</sup>

Hernan Terenzi,<sup>§,||</sup> Pedro M. Alzari,<sup>⊥</sup> and Mario M. Zakin<sup>\*,§</sup>

*Unité d'Expression des Gènes Eucaryotes and Unité de Biochimie Structurale, Institut Pasteur, 25/28 rue du Dr. Roux, 75724 Paris Cedex 15, France*

*Received April 2, 1998; Revised Manuscript Received June 23, 1998*

**ABSTRACT:** The nuclear receptor superfamily comprises a group of transcriptional regulators involved in a wide variety of physiological responses. Rev-erb $\beta$  is a member of a growing subfamily of orphan nuclear receptors that bind DNA with high affinity either as monomers or as hetero- or homodimers. DNA bending assays, high-resolution footprinting, molecular modeling, and site-directed mutagenesis were used to analyze the structural features of the interaction between the DNA-binding domain (DBD) of the nuclear receptor Rev-erb $\beta$  and its DNA target sites. The results obtained point to the involvement of a carboxyl-terminal sequence adjacent to the second zinc finger of the Rev-erb $\beta$  DBD in protein–DNA interaction as a monomer or in protein–DNA and protein–protein interactions as a homodimer. They also provide insight about the amino acid residues directly involved in protein–protein contacts.

The members of the superfamily of nuclear receptors are transcription factors interacting with specific DNA sequences known as hormone response elements (HREs)<sup>1</sup> (1). These proteins contain a highly conserved region of about 70 amino acid residues which includes two class II zinc fingers required for specific binding to the HREs (2–5). Typically, nuclear receptors interact as homo- or heterodimers with sequences composed of two direct or inverted copies of a six-nucleotide element of the form AGAACA or AGGTCA separated by a variable number of nucleotides (6, 7). However, not all nuclear receptors interact with DNA as dimers. An increasing number of orphan receptors have been demonstrated to bind to DNA as monomers. In these cases, the core motif recognized by the DNA-binding domain (DBD) contains a single AGGTCA motif preceded by two adenines or by a 5 or 6 bp A/T-rich sequence (8–10). Crystal structure and nuclear magnetic resonance (NMR) analysis of glucocorticoid (GR) and estrogen (ER) receptor DBDs (2–5) show that the two zinc finger motifs form a single structural unit implicated in both protein–DNA and protein–protein in-

teractions. According to these structures, a pair of amphipathic  $\alpha$ -helices are packed at right angles, with a zinc-binding pocket lying at the N terminus of each helix. NMR studies of a 94-residue retinoic X receptor (RXR) DBD show that the overall fold of this polypeptide is similar to that of the GR and ER DBDs, with the exception that RXR has an additional C-terminal  $\alpha$ -helix which is required for high-affinity DNA binding and serves as a dimerization interface for protein–protein interactions (11). In some other receptors interacting with DNA as monomers, a C-terminal region known as the T and A boxes, immediately adjacent to the second zinc finger domain as the C-terminal RXR DBD helix, has also been suggested to be involved in contacts with DNA. Moreover, different analyses suggest that this region is essential for the recognition of the 5' extension of monomeric HREs (12–14).

Rev-erb $\beta$  is a transcription factor with a molecular mass of about 64 kDa that belongs together with Rev-erb $\alpha$  and ROR/RZR $\alpha$  to an orphan ligand subgroup of the nuclear receptor superfamily. Its mRNA was found in several organisms (15–19), and the Rev-erb $\beta$  gene has been located in mouse chromosomes 19 and 14 (20). The protein seems to act as a constitutive negative regulator of transcription, competing with other nuclear receptors such as the ROR $\alpha$  isoforms for an overlapping network of responsive elements (21). We have recently demonstrated that, as observed with Rev-erb $\alpha$  (22), the Rev-erb $\beta$  DBD (REDBD) interacts as a monomer with oligonucleotides containing an A/T-rich sequence preceding a single AGGTCA site (Rev-RE15) or as a homodimer with an AGGTCA direct repeat separated by 2 bp (Rev-DR2) (23). In the latter case, a minority of monomeric complexes can be detected in electrophoretic mobility shift assays (EMSA) (23; see Figure 7B, lane 2). To our knowledge, the Rev-erb proteins constitute the first

<sup>†</sup> This work was supported by the Centre National de la Recherche Scientifique (URA 1129) and by the Commission of the European Communities (CEC Contract BIO2-CT93-0319).

<sup>‡</sup> This paper is dedicated to the memory of our dear friend Prof. J. C. da Costa Maia.

<sup>\*</sup> To whom correspondence should be addressed. Telephone: 33 1 45688382. Fax: 33 1 40613110. E-mail: mzakin@pasteur.fr.

<sup>§</sup> Unité d'Expression des Gènes Eucaryotes.

<sup>||</sup> Present address: Departamento de Bioquímica, CCB-UFSC, 88040-900 Florianópolis, Brazil.

<sup>⊥</sup> Unité de Biochimie Structurale.

<sup>1</sup> Abbreviations: HREs, hormone response elements; DBD, DNA-binding domain; GR, glucocorticoid receptor; ER, estrogen receptor; RXR, 9-cis retinoic acid receptor; TR, thyroid hormone receptor; REDBD, Rev-erb $\beta$  DNA-binding domain; DR2, tandem of half-sites AGGTCA separated by 2 bp; DR4, tandem of half-sites AGGTCA separated by 4 bp; EMSA, electrophoretic mobility shift assay.

model accounting for nuclear receptors interacting with DNA either as monomers or as homodimers. In this paper, DNA bending assays, high-resolution footprinting, molecular modeling, and site-directed mutagenesis allowed us to examine in more detail how REDBD interacts with DNA. Our results demonstrate that the C-terminal region adjacent to the second zinc finger motif is essential for the interaction of REDBD with DNA as a monomer, and is responsible for the phenomenon of cooperative dimeric binding to the corresponding DNA target site.

## EXPERIMENTAL PROCEDURES

**Overexpression and Purification of REDBD.** As previously described (23), the DH5 $\alpha$  bacteria transformed with pDRE, a pGEX-2T-REDBD vector, were grown in LB medium supplemented with ampicillin at 0.1 mg/mL, to an absorbance of 0.5 at 600 nm. They were then induced with 1.0 mM IPTG for 4 h at 37 °C under good aeration. Cells were harvested by centrifugation at 6000g. The pellet from 1000 mL of culture was suspended in 20 mL of phosphate-buffered saline (PBS) with 5 mM phenylmethanesulfonyl fluoride (PMSF), 1 mM dithiothreitol (DTT), 0.5  $\mu$ g/mL leupeptin, 0.7  $\mu$ g/mL pepstatin, and 40  $\mu$ g/mL bestatin. The cells were disrupted by gentle sonication (four cycles/20 s) in ice; Triton X-100 was added to a final concentration of 1% and the suspension centrifuged for 20 min at 15000g. The supernatant was incubated overnight at 4 °C with 2 mL of glutathione-Sepharose (Pharmacia). The resin was washed with 15 volumes of PBS and finally with thrombin cleavage buffer [50 mM Tris-HCl (pH 8), 150 mM NaCl, and 2.5 mM CaCl<sub>2</sub>]. Thrombin was added [approximately 0.05% (w/v)] and incubation performed for 2 h at room temperature. The cleaved protein was washed out by addition of 50 mM Tris-HCl (pH 8), 400 mM NaCl, 5 mM MgCl<sub>2</sub>, 1 mM DTT, and 10% glycerol and applied to a heparin-Sepharose column connected to a FPLC system (HiTrap 5 mL, Pharmacia) after dilution to 50 mM NaCl. The column was submitted to a linear elution gradient from 50 to 1 M NaCl, in 5 column volumes; the protein was eluted at 400 mM NaCl, and purified fractions were concentrated by ultrafiltration with Centricon 3 (Amicon) membranes. The concentration of protein was calculated (24), and fractions corresponding to each purification step were analyzed by SDS-PAGE; the gels were stained with Coomassie Brilliant Blue G-250.

**Size Exclusion Chromatography.** To calculate the relative molecular mass of native REDBD in solution, a Superdex-200 column (Pharmacia) was used following the manufacturer's recommendations. A 25  $\mu$ L sample of a 1 mM solution of REDBD in 50 mM Tris-HCl buffer (pH 8), 0.2 M NaCl, 5 mM MgCl<sub>2</sub>, 1 mM DTT, and 10  $\mu$ M ZnSO<sub>4</sub> was applied to the column connected to a FPLC system, at 0.4 mL/min. The elution of REDBD was detected at 280 nm and also by SDS-PAGE analyses of the fractions. A mixture of gel filtration molecular mass markers (BSA, 67 kDa; ovalbumin, 43 kDa; chymotrypsinogen, 25 kDa; and RNase A, 13.7 kDa) was used to obtain a calibration curve under the same elution conditions of REDBD.

**Circular Permutation Assay.** In a final volume of 20  $\mu$ L, 1  $\mu$ g of pBEND3 (25)-Rev-RE15 or -Rev-DR2 digested by different restriction enzymes, 2  $\mu$ L of 0.1 M Tris-HCl

(pH 8.0), 50% glycerol, 5  $\mu$ L of 4 mM DTT, 0.04% NP40, 0.4 mM EDTA, 0.6 M NaCl, 20 mM MgCl<sub>2</sub>, and REDBD in concentrations ranging from 0 to 5  $\mu$ M were incubated at 4 °C over the course of 30 min and immediately applied to a 6% acrylamide nondenaturing gel, and electrophoresis was run for 2 h at 4 °C. The DNA-protein complex was revealed by ethidium bromide staining.

**DNase I Footprinting.** The top strand of the analyzed fragment was obtained by *Eco*RI digestion of the pBEND3 plasmid used for bending experiments (25), and the 3' extremity was labeled using Klenow polymerase in the presence of <sup>32</sup>P-labeled  $\alpha$ -dATP. The bottom strand was obtained by digestion with *Hind*III of the same plasmid, followed by treatment with Klenow polymerase in the presence of <sup>32</sup>P-labeled  $\alpha$ -dATP. In both cases, the fragments were purified on a 6% polyacrylamide gel. About 50 000 cpm of the probes (8 fmol) was mixed with REDBD (0–2000 nM protein) and 2  $\mu$ L of a 10 $\times$  binding buffer [100 mM Tris-HCl (pH 8), 600 mM NaCl, 50% glycerol, 10 mM DTT, and 50 mM MgCl<sub>2</sub>] in a final volume of 20  $\mu$ L. After incubation for 30 min at room temperature, 1 unit of DNase I was added and the reaction was stopped after incubation for 120 s at room temperature by adding 500  $\mu$ L of the DNase stop solution [50 mM EDTA, 0.2% (w/v) SDS, and 100  $\mu$ g/mL tRNA]. After a phenol/chloroform extraction, the mixtures were precipitated with ethanol and the pellets resuspended with a formamide-containing dye and incubated for 2 min at 90 °C. Then the reaction samples were loaded onto a 6% sequencing gel, which was run for 75 min at 75 W. The gel was dried and exposed for autoradiography. Chemical sequencing reactions were carried out according to the Maxam-Gilbert method.

**Ferrous-EDTA Footprinting.** The probes and the binding conditions were exactly the same as those used for DNase I footprinting. After REDBD binding to the probe, the hydroxyl radicals were generated by the addition of 2  $\mu$ L of a fresh aqueous 40 mM [Fe(EDTA)]<sup>2-</sup> solution, 2  $\mu$ L of 40 mM ascorbate, and 2  $\mu$ L of 2% H<sub>2</sub>O<sub>2</sub>. The reactions were stopped by adding 5  $\mu$ L of a 0.5 M thiourea solution. Analyses of the samples were as described for the DNase I footprinting protocol, and the footprinting patterns were analyzed by comparing the densitometric profiles using Molecular Dynamics software.

## RESULTS

**REDBD Is a Monomer in Solution.** We have previously demonstrated that a monomeric or a dimeric form of REDBD is capable of recognizing a single (Rev-RE15) or a direct repeat (Rev-DR2) of the nuclear receptor DNA consensus sequence AGGTCA (23). The primary sequence of REDBD and the DNA sequences of Rev-RE15 and Rev-DR2 are presented in Figure 1. To determine its free oligomerization state in solution, a 95% homogeneous preparation of REDBD (Figure 2, lane 3) was analyzed by gel filtration chromatography in a Superdex-200 column. Under our experimental conditions, we observed that the preparation eluted as a single peak, corresponding to a globular protein of 14 kDa (Figure 3). This result is consistent with the molecular mass of the protein as determined by electrospray ionization mass spectrometry (12.615 kDa) (data not shown) or as predicted from the sequence (17–19, 21; Figure 1). This indicates that REDBD exists as a monomer in solution.

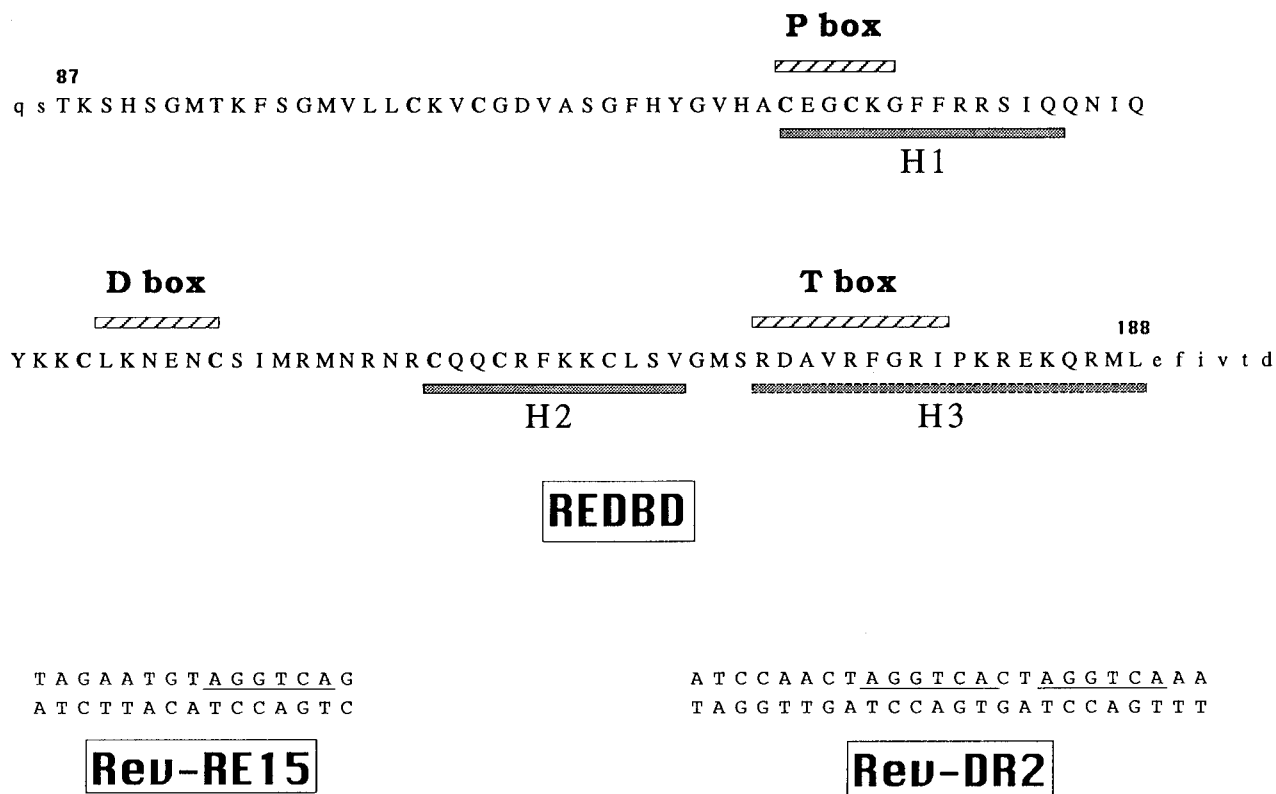


FIGURE 1: Amino acid sequence of REDBD residues 87–188 and DNA sequences of Rev-RE15 and Rev-DR2. Hypothetical  $\alpha$ -helices are indicated by H1–3. Amino acids in the P box are important for DNA recognition. The D box is involved in phosphate contacts and dimerization in the GRs and ERs. The T box is a domain homologous to that involved in the formation of RXR homodimers. The AGGTCA half-sites are underlined in the Rev-RE15 and Rev-DR2 sequences.

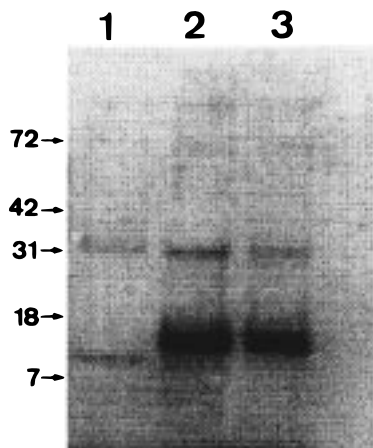


FIGURE 2: SDS-PAGE of truncated (residues 85–175), mutant (residues 87–188, F176S and I179S), and wild type (residues 87–188) REDBD proteins. An aliquot of 10  $\mu$ L of each purification batch of the proteins described above was loaded on a 10% polyacrylamide gel (lanes 1–3, respectively). At the extreme left, the molecular mass markers are indicated.

**REDBD Induces a DNA Bend in the Direct Repeat Rev-DR2 Binding Site.** To determine whether REDBD induces DNA bending at its Rev-RE15 and Rev-DR2 recognition sites, we have performed a circular permutation analysis (25) which is a method capable of detecting subtle changes in DNA structure such as those induced by protein binding. We cloned the Rev-RE15 and Rev-DR2 targets in the pBEND3 vector (25), obtaining the different probes by positioning each target site at the end or at the middle of the probe by means of restriction enzyme digestion (Figure 4). If a bend is introduced upon DNA–protein complexation,

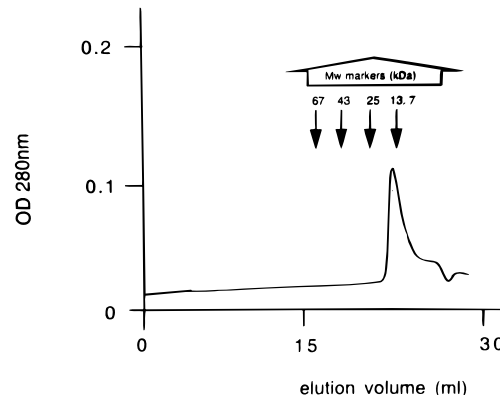


FIGURE 3: REDBD is a monomer in solution. The relative molecular mass of native REDBD in solution was determined by using gel filtration chromatography (Superdex-200 column).

the probe with the target in the middle migrates slower than that with the target located at the extremities in an electrophoretic mobility shift assay (EMSA). The difference in the relative migration of the complexes in the gel provides a rough estimate of the bending angle. For REDBD, a bend angle of  $38^\circ$  was observed with the Rev-DR2 target, but no significant migration differences were observed under our experimental conditions with the Rev-RE15 motif (Figure 4). If the entire protein interacts with DNA in a manner similar to that of its DBD fragments, we could expect different physiological responses in vivo when Rev-erb $\beta$  binds as a monomer or as a dimer.

**Identification of Nucleotide Regions Contacting REDBD in the Monomeric or Dimeric Complexes.** The footprinting technique (26–28) is used to detect the DNA regions



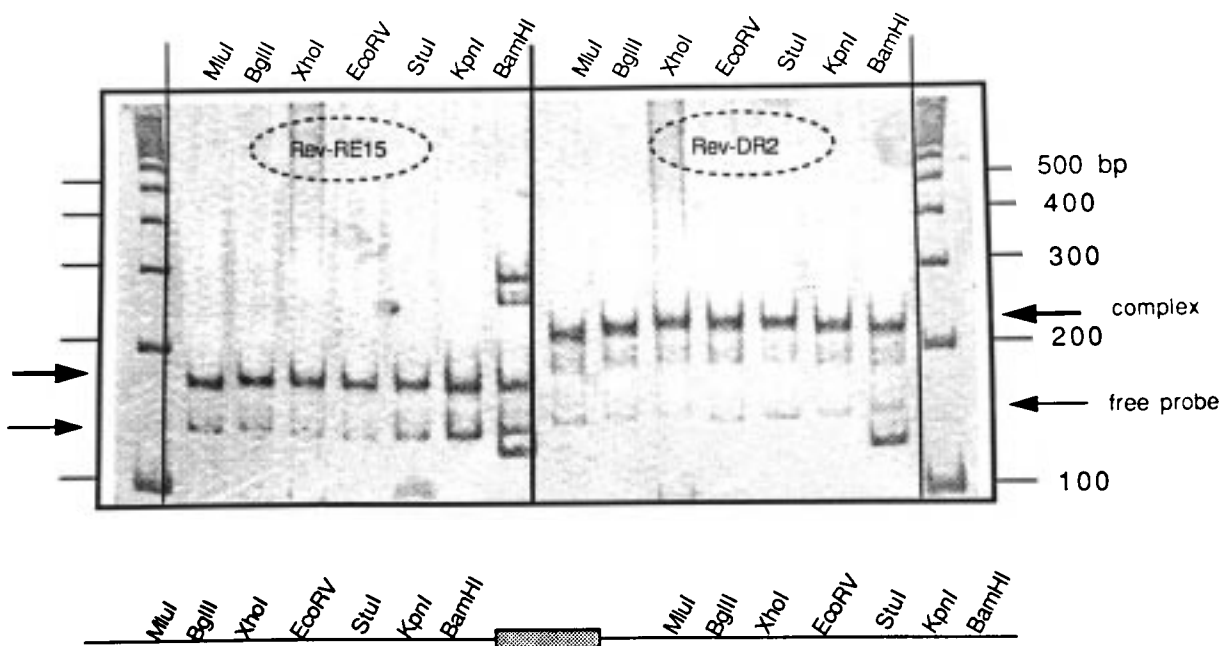


FIGURE 4: REDBD promotes a 38° bend in the Rev-DR2 probe but does not seem to bend the Rev-RE15 probe. Circular permutation assays were performed using the Rev-RE15 or the Rev-DR2 sequences cloned in the pBEND-3 plasmid. Each probe was obtained by using one of the restriction sites indicated in the scheme presented in the lower part of the figure.

important for binding by a protein or a chemical substance. We performed DNase I footprinting to detect the positioning of REDBD when it interacts with Rev-RE15 or with Rev-DR2 (Figure 5A, upper and lower panels, respectively). The protections obtained for either the upper (+) or lower (−) strand of the two DNA sequences are summarized in Figure 6. The Rev-RE15 (+) strand is protected in 21 positions, while the Rev-RE15 (−) strand in only 17. In contrast, 29 nucleotides are protected in the Rev-DR2 (+) strand and 23 in the Rev-DR2 (−) strand, clearly showing the larger surface occupied by the REDBD homodimer. These data indicate the tight binding of REDBD to its DNA target sites. Furthermore, they suggest for this monomer in solution a cooperative binding to Rev-DR2, since no half-occupancy of the DNA probe is observed under our footprinting conditions, confirming our previous results (23). The 5′ A/T-rich sequences found upstream of the AGGTCA site, which were shown to be important for the binding of a homologous nuclear receptor DBD (9), are clearly protected from DNase I cleavage in Rev-RE15 and Rev-DR2, suggesting that this region plays a similar important role in REDBD–DNA binding events.

However, since DNase I is an enzyme of approximately 30 kDa, the size of the protected regions is rather overestimated from the information obtained from the corresponding footprinting technique, mainly because of steric hindrance between the enzyme and the DNA binding protein. Therefore, to obtain a more accurate pattern of the bases interacting with REDBD, we decided to use the hydroxyl radical footprint (27, 28). In Rev-RE15, we observed two regions protected in each strand (Figure 5B, upper panel). The 5′ or 3′ extremities of each region are separated from the corresponding extremities of the other region by around 10 nucleotides, which is the step of the DNA helix in normal B-DNA structure. The modulation of the intensity of the bands with a regular phasing according to the helix repeat strongly suggests the binding of the protein to one side of

the DNA (28). An almost similar protection pattern was observed with Rev-DR2 (Figure 5B, lower panel), but in this case with three protected regions separated roughly by 9 to 10 nucleotides. Thus, the homodimer also seems to face mostly one side of the B-DNA target as the monomer does, and a similar shift between upper (+) and lower (−) strands is observed. The protections obtained for either the upper (+) or lower (−) strand of the two DNA sequences are summarized in Figure 6.

**Model Construction of REDBD–Rev-DR2 and Site-Directed Mutagenesis in the C-Terminal Region of REDBD.** As revealed by EMSA, a C-terminal truncated mutant of REDBD bearing residues 87–175 (Figure 2, lane 1) was unable to bind DNA either as a monomer or as a dimer (lane 6 of Figure 7A and lane 6 of Figure 7B, respectively). A weak binding of the truncated protein was observed with Rev-RE15 that corresponds only to less than 5% of the wild type protein binding. This indicated that the two zinc-binding motifs of REDBD are not sufficient for protein interaction with DNA and that the REDBD C-terminal portion is essential for this interaction. The sequence of the deleted region (amino acid residues 176–188) is homologous to the corresponding regions of Rev-erb $\alpha$  and ROR $\alpha$  isoforms and to the sequence of the C-terminal helix of RXR adjacent to the second zinc finger motif (29). It has been shown that this helix mediates both protein–protein and protein–DNA interactions necessary for the cooperative dimeric binding of the RXR DBD to its target site, an AGGTCA direct repeat separated by one base pair (DR1 DNA) (11).

A homology model of the REDBD–Rev-DR2 complex (Figure 8B) based on the crystal structure of the heterodimer RXR-TR bound to a DR4 DNA (Figure 8A) (30) suggests that the T and A box region of REDBD immediately following the second zinc finger domain might fold into a helix, consistent with secondary structure predictions (see Figure 1). As a consequence, a pair of hydrophobic side

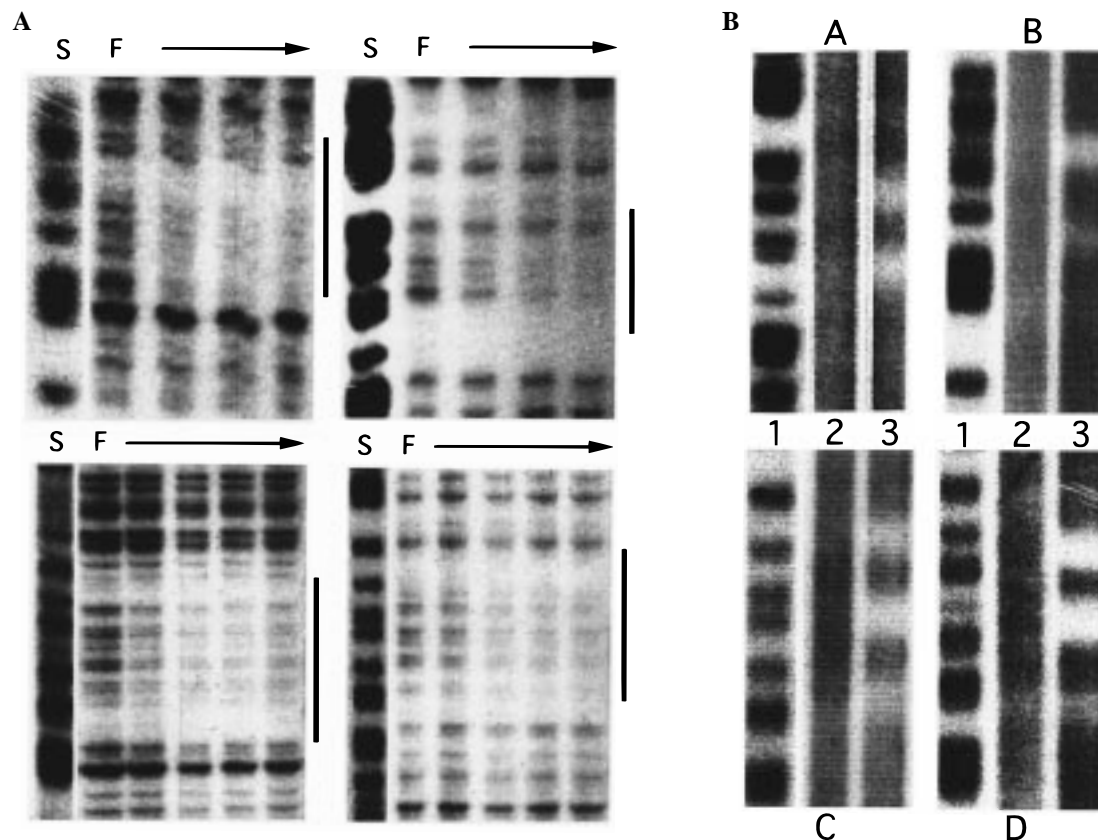


FIGURE 5: (A) DNase I footprint analysis. In each panel, the patterns of protection in Rev-RE15 (+ or – strand, left upper panel or right upper panel, respectively) and in Rev-DR2 (+ or – strand, left lower panel or right lower panel, respectively) in the presence of REDBD are shown. A range of protein concentration of 0–2000 or 0–500 nM was used to titrate the Rev-RE15 and Rev-DR2 probes, respectively (horizontal arrows). Vertical lines delineate sequences protected against DNase I digestion. S represents chemical cleavages at purine residues (G and A); F represents the free DNA assay where no REDBD was added. (B) Hydroxyl radicals as footprinting probes. In each panel, the patterns of protection in Rev-RE15 (+ or – strand, lane 3 of the right upper panel or lane 3 of the left upper panel, respectively) and in Rev-DR2 (+ or – strand, lane 3 of the right lower panel or lane 3 of the left lower panel, respectively) in the presence of REDBD are shown. The REDBD concentration used was 1000 nM: lanes 1, chemical cleavages at purine residues (G and A); and lanes 2, free DNA assay where no REDBD was added.

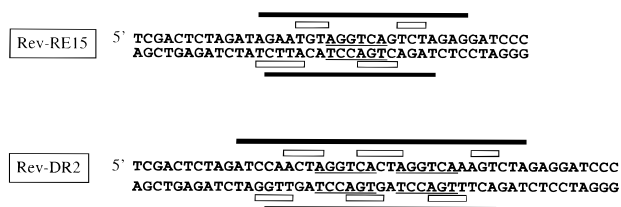


FIGURE 6: Summary of DNA–protein contacts obtained from DNase I and ferrous-EDTA footprintings. Solid bars indicate the contacts detected in the DNase I footprints and open bars those detected in the hydroxyl radical footprints. The sequence AGGTCA and its complementary sequence are underlined.

chain residues, Phe176 and Ile179, separated by one helical turn, would be favorably oriented to participate in protein–protein interactions (Figure 8B). To test this hypothesis, the two amino acid residues were changed to serine by site-directed mutagenesis. As indicated by EMSA (Figure 7), the mutant REDBD protein (Figure 2, lane 2) conserved the capability to bind DNA as a monomer (suggesting that these two residues are not involved in DNA contacts) (Figure 7A,B, lanes 4) but failed to form the dimeric REDBD–Rev-DR2 complex (Figure 7B, lane 4). These results further confirm the involvement of the C-terminal region of REDBD in protein–protein interactions and appear to validate the hypothesis based on the molecular model, providing some insight about the amino acid residues directly involved in

protein contacts. Thus, the site-directed mutagenesis experiments and the assays with truncated proteins showed that the C-terminal portion of REDBD is involved in both protein–protein and protein–DNA interactions.

## DISCUSSION

Members of the nuclear receptor superfamily interact with the AGGTCA DNA sequences via different mechanisms. At least three subgroups of these proteins can be defined: those that bind DNA as homodimers, as heterodimers with the RXR receptor, or as monomers.

Structural studies showed that the ER and GR DBDs binding as homodimers to HRE half-sites oriented as inverted repeats contain in their two zinc-binding motifs all the elements for interacting with their DNA target sites (2–5). In contrast, the RXR DBD contains an additional helix after the second zinc finger, required for selective dimerization of the RXR DBD on HREs composed of AGGTCA half-sites arranged as direct repeats (11). More recently, the crystal structure of the complex formed by the RXR and the TR DBDs bound to a TR HRE (DR4 DNA) also showed that the subunits interact through a DNA-supported interface involving the C-terminal DBD element of the TR nuclear receptor (30).

ROR $\alpha$  isoforms interact as monomers with an HRE named RORE composed of a 5' A/T-rich sequence preceding the

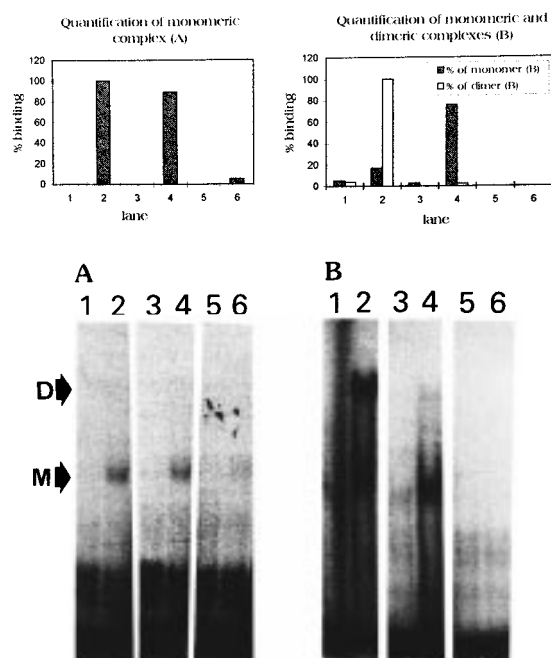


FIGURE 7: C-Terminal region (residues 176–188) of REDBD essential for DNA–protein interaction and amino acid residues Phe176 and Ile179 essential for protein–protein interactions. EMSAs were performed using Rev-RE15 in panel A and Rev-DR2 in panel B. In lanes 1, 3, and 5, no protein was added. In lanes 2, 4, and 6, 200 ng of protein was used. In lane 2, wild type REDBD was used. In lane 4 in mutated REDBD, Phe176 and Ile179 were replaced by Ser. In lane 6, a C-terminal truncated protein bearing residues 87–175 was used. Above each panel is a histogram representing the densitometric analysis of the DNA–protein complexes. In panel A, 100% refers to the optical density of the monomeric complex in lane 2. In panel B, 100% refers to the optical density of the dimeric complex in lane 2.

AGGTCA hexamer (10). Site-directed mutagenesis and domain swap experiments have indicated that orphan nuclear receptors as these isoforms or as NGFI-B interact with the 5' extension of their monomeric HREs binding site through a distinct subdomain of their DBD, referred to as the T and A boxes. This subdomain is located, as the additional  $\alpha$ -helix of the RXR DBD (11), in a C-terminal region adjacent to the second zinc-binding motif. Methylation and ethylation interference and site-directed mutagenesis experiments suggest that the ROR $\alpha$  DBD is bipartite, with the two zinc-binding motifs contacting the major groove at the 3' AGGTCA sequence, and the C-terminal element interacting along the same face of the DNA helix with the adjacent minor groove at the 5' A/T-rich sequence. Restriction enzyme digestions leading to truncated proteins and point mutations assays also showed that the integrity of the carboxyl-terminal element and of the Arg148 situated in this region are essential for the binding of the ROR $\alpha$  DBD to its target site RORE (29).

The Rev-erb DBD sequences are homologous to the corresponding regions of ROR $\alpha$  isoforms. Recently, we and others have demonstrated that the Rev-erb nuclear receptors bind as monomers to Rev-RE, an HRE similar to RORE, but also as homodimers to their monomer binding site separated by 2 bp from another AGGTCA sequence (22, 23). To our knowledge, the Rev-erb proteins constitute the first model accounting for a nuclear receptor interacting with the DNA either as a monomer or as a homodimer.

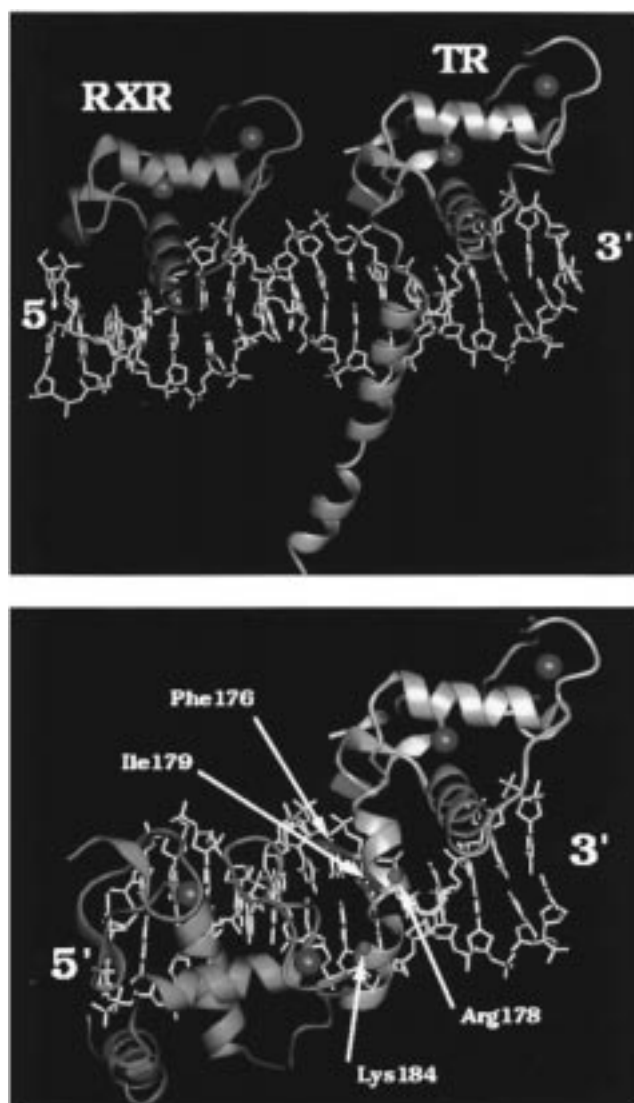


FIGURE 8: (A, top) RXR (red) and TR (blue) DBDs interacting with the TRE DR4 DNA as observed in the crystal structure. (B, bottom) The REDBD homodimer interacting with Rev-DR2 DNA as predicted by molecular modeling. Amino acid residues Phe176 and Ile179, which are essential for protein–protein interactions between the REDBD monomers, and the C $\alpha$  positions of Arg178 and Lys184, suggested to be involved in DNA–protein interactions, are indicated.

To determine the structural features of REDBD that promote binding to its DNA targets Rev-RE15 and Rev-DR2, we have used DNA bending assays, high-resolution footprinting, molecular modeling, and site-directed mutagenesis and we have also taken into account previous results obtained with other related nuclear receptor models.

To model the REDBD dimer bound to the B-form of DNA for visualization purposes, the protein–protein interface seen in the crystal structure of the RXR-TR DBDs–DR4 DNA complex (30; PDB code 2NLL) was adjusted by reducing the number of spacers by 2 bp. If one REDBD monomer is positioned as TR in the heterodimer, the other REDBD monomer is rotated 70° and displaced 7 Å along the B-DNA axis with respect to the RXR DBD (Figure 8). The assumption of a similar mode of binding of the core REDBD to DNA is validated by the nearly identical conformation and alignment with respect to DNA observed in all known structures of nuclear receptor DBDs (11).



The REDBD-DR2 model also respects the critical contacts observed between the C-terminal  $\alpha$ -helix of TR and the minor groove of DNA in the RXR-TR-DR4 complex (30). In particular, the C-terminal helix of TR DBD contains a critical Lys residue (Lys80 in the three-dimensional structure of TR DBD, corresponding to Lys184 in REDBD) which makes several contacts with the phosphate backbone and nucleotides within the minor groove of DNA. Indeed, these contacts made by the C-terminal region of REDBD are critical for the protein to bind as a monomer, since the deletion of REDBD residues 176–188 precludes binding to Rev-RE15 (see above and lane 6 of Figure 7A).

In TR DBD, the T box segment forms a connecting loop containing a one-turn  $3_{10}$ -helix and is followed by a long C-terminal  $\alpha$ -helix, corresponding to the A box region of NGFI-B, a nuclear receptor interacting with the DNA as a monomer or as a heterodimer with RXR (8, 13, 31). This  $\alpha$ -helix makes critical contacts with the DNA backbone and with functional bases in the minor groove. Compared with TR, REDBD has an insertion of one amino acid residue within the T box region. This insertion can be accommodated in the three-dimensional model without affecting the orientation of the DBD or the position of the C-terminal  $\alpha$ -helix by modeling the T box region as a second helix, i.e., extending the one-turn  $3_{10}$ -helix observed in TR. This model would imply that the entire C-terminal region of REDBD folds into a long helix disrupted by the presence of a proline residue (Pro180) which separates approximately the T box from the A box (Figure 8B). Some evidence appears to support this model. (a) Methods of secondary structure prediction indicate the presence of two helical regions separated by a proline in the sequence beyond the second zinc finger domain (H3, Figure 1). (b) A helical T box region would be consistent with the NMR structure of RXR (11). Indeed, the failure to observe this helix in the RXR-TR-DR4 crystal structure could be due to the fact that it is not stabilized by protein-protein interactions (since RXR binds to the upstream half-site) and that RXR is not able to bind DNA as a monomer. (c) A helical T box as modeled predicts that two hydrophobic side chain residues, Phe176 and Ile179, would be positioned in the outer face of the helix and would be involved in protein-protein interactions, but not in protein-DNA interactions. As shown above, mutation of these residues into serine precludes binding of REDBD as a dimer, but the protein is still capable of binding as a monomer (Figure 7B, lane 4), thus apparently validating the model prediction. (d) In contrast to Phe176 and Ile179, Arg178 would be positioned in the inner face of the helix (Figure 8B), thus likely pointing toward DNA. As indicated before, in ROR $\alpha$ , the equivalent arginine residue (Arg148) was shown to be essential for the binding of the protein to its DNA target site (29).

If a similar mode of interaction of each DBD with the major groove of DNA is assumed, the most significant difference between the DR4 and DR2 complexes involves the relative orientation of the two protein domains. In DR4, RXR and TR bind to the same face of the DNA in such a way that the second zinc finger domain and the T box region of one DBD interact with the first zinc finger domain of the second DBD (Figure 8A). Instead, a spacer of two base pairs (DR2) implies a relative rotation of the protein domains which promotes contacts between the C-terminal region (but

not the second zinc finger domain) of the DBD domain bound to the second half-site and the helix-connecting loop forming the first zinc finger of the 5' DBD (Figure 8B).

The model is also compatible with the protection results observed in nucleotides contacting the DBD core (Figures 5 and 6). Protected bases upstream of the 5' half-site AGGTCA could correspond to the contacts of the C-terminal region of REDBD with the A/T-rich region. These interactions are expected to provide the increase in affinity necessary for REDBD to bind as a monomer, in a similar way as proposed for TR, NGFI-B, and ROR $\alpha$  (29).

The DNA bending observed in circular assays for Rev-DR2 could indicate an important difference in the mode of binding compared with that for DR4, since in this case the complexed B-DNA showed no significant bending (30). When the REDBD homodimer is modeled bound to linear unbent B-DNA (as shown in Figure 8), the model suggests intimate contacts at the interface between the two REDBD monomers which could account for the observed bending of the DNA. Indeed, the C-terminal region of nuclear receptor DBDs has already been proposed to play a steric role in spacer discrimination on the basis of the RXR-TR crystal structure (30) and of in vitro affinity studies with chimeric DBDs in which the C-terminal region has been interchanged between distinct nuclear receptors (29).

In conclusion, the study presented here gives us a greater appreciation of the molecular mechanisms involved in the interaction of a nuclear receptor DBD capable of interacting with the DNA as a monomer or as a homodimer. The results obtained and those previously reported with other models point to a general role played by the C-terminal extension of the polypeptide, which seems to be essential to achieving specific and stable DNA binding of nuclear receptor DBDs acting as monomers, homodimers, or heterodimers.

## ACKNOWLEDGMENT

We thank G. N. Cohen and B. Baron for critical reading of the manuscript and O. Barzu and A. Namane for performing the mass spectrometry experiments.

## REFERENCES

1. Yamamoto, K. R. (1985) *Annu. Rev. Genet.* 19, 209–252.
2. Härd, T., Kellenbach, E., Boelens, R., Maler, B. A., Dalhman, K., Freedman, L. P., Carlstedt-Duke, J., Yamamoto, K. R., Gustafsson, J.-A., and Kaptein, R. (1990) *Science* 249, 157–160.
3. Schwabe, J. W. R., Neuhaus, D., and Rhodes, D. (1990) *Nature* 340, 458–461.
4. Luisi, B. F., Xu, W. X., Otwinowski, Z., Freedman, L. P., Yamamoto, K. R., and Sigler, P. B. (1991) *Nature* 352, 497–505.
5. Schwabe, J. W. R., Chapman, L., Finch, J. T., and Rhodes, D. (1993) *Cell* 75, 567–578.
6. Evans, R. M. (1988) *Science* 240, 889–895.
7. Umesono, K., Murakami, K. K., Thompson, C. C., and Evans, R. M. (1991) *Cell* 65, 1255–1266.
8. Wilson, T. E., Fahrner, T. J., Johnston, M., and Milbrandt, J. (1991) *Science* 252, 1296–1300.
9. Harding, H. P., and Lazar, M. A. (1993) *Mol. Cell. Biol.* 13, 3113–3121.
10. Giguère, V., Tini, M., Flock, G., Ong, E. S., Evans, R. M., and Otulakowski, G. (1994) *Genes Dev.* 8, 538–553.

11. Lee, M. S., Kliewer, S. A., Provençal, J., Wright, P. E., and Evans, R. M. (1993) *Science* 260, 1117–1121.
12. Ueda, H., Sun, G. C., Murata, T., and Hirose, S. (1992) *Mol. Cell. Biol.* 12, 5667–5672.
13. Wilson, T. E., Paulsen, R. E., Padgett, K. A., and Milbrandt, J. (1992) *Science* 256, 107–110.
14. Wilson, T. E., Fahrner, T. J., and Milbrandt, J. (1993) *Mol. Cell. Biol.* 13, 5794–5804.
15. Enmark, E., Kainu, T., Pelto-Huikko, M., and Gustafsson, J. A. (1994) *Biochem. Biophys. Res. Commun.* 204, 49–56.
16. Dumas, B., Harding, H. P., Choi, H. S., Lehmann, K. A., Chung, M., Lazar, M. A., and Moore, D. D. (1994) *Mol. Endocrinol.* 8, 996–1005.
17. Retnakaran, R., Flock, G., and Giguère, V. (1994) *Mol. Endocrinol.* 8, 1234–1244.
18. Bonnelye, E., Vanacker, J. M., Desbiens, X., Bègue, A., Stéhelin, D., and Laudet, V. (1994) *Cell. Growth Differ.* 5, 1357–1365.
19. Giambiagi, N., Cassia, R., Petropoulos, I., Part, D., Cereghini, S., Zakin, M. M., and Ochoa, A. (1995) *Biochem. Mol. Biol. Int.* 37, 1091–1102.
20. Cassia, R., Mattei, M. G., Jaubert, J., Poirier, C., Giambiagi, N., Ochoa, A., and Zakin, M. M. (1996) *Mamm. Genome* 7, 243.
21. Forman, B. M., Chen, J., Blumberg, B., Kliewer, S. A., Henshaw, R., Ong, E., and Evans, R. M. (1994) *Mol. Endocrinol.* 8, 1253–1261.
22. Harding, H. P., and Lazar, M. A. (1995) *Mol. Cell. Biol.* 15, 4791–4802.
23. Terenzi, H., Cassia, O. R., and Zakin, M. M. (1996) *Protein Expression Purif.* 8, 313–318.
24. Bradford, M. M. (1976) *Anal. Biochem.* 72, 48–54.
25. Zwieb, C., and Adhya, S. (1994) in *DNA-Protein Interactions* (Kneale, G., Ed.) pp 281–294, Humana Press, Totowa, NJ.
26. Leblanc, B., and Moss, T. (1994) in *DNA-Protein Interactions* (Kneale, G., Ed.) pp 1–10, Humana Press, Totowa, NJ.
27. Tullius, Th. D., Dombrosky, B. A., Churchill, M. E. A., and Kam, L. (1987) *Methods Enzymol.* 155, 537–558.
28. Schickor, P., and Heumann, H. (1994) in *DNA-Protein Interactions* (Kneale, G., Ed.) pp 21–32, Humana Press, Totowa, NJ.
29. Giguère, V., McBroom, L. D. B., and Flock, G. (1995) *Mol. Cell. Biol.* 15, 2517–2526.
30. Rastinejad, F., Perlmann, T., Evans, R. M., and Sigler, P. B. (1995) *Nature* 375, 203–211.
31. Perlmann, T., and Jansson, L. (1995) *Genes Dev.* 9, 769–782.

BI980748I